Journal of Hydraulic Structures
J. Hydraul. Struct., 2021; 7(3):59-71
DOI: 10.22055/jhs.2021.37998.1182

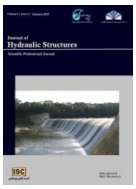

OPEN ACCESS

Application of SSIIM numerical model in simulation of local scouring around the aerodynamic bridge pier located in 90 ° bend

Mousa Rasaei [1]
Siavash Kolbi [2]

Abstract

Bridges are one of the most important and widely used river structures. Every year, a large number of them are destroyed by factors such as scouring and erosion. It is sometimes observed that the bridges are placed in the river bend, due to restrictions such as the road construction or river instability. On the other hand, studies have shown that the geometric shape of the bridge pier will have significant effect on the depletion of flow energy and thus reduce the scour depth around the bridge pier. Therefore, in this study, the effect of bend angle changes on flow pattern and local scouring around the of cylindrical bridge piers with aerodynamic shapes were investigated. SSIIM Three-dimensional software was used for modeling. The results showed that by increasing the bend angle and also placing the pier with a wide nose upstream, the amount of depth and volume of scouring increases, so that, the maximum depth and volume of scour occurred at a 90-degree angle to 0.1197123 m and 0.08436892 cubic meters, respectively.

Keywords: Bend Angle, Local Scouring, Bridge Pier, Aerodynamic Shape, SSIIM Numerical Model.
Received: 17 July 2021; Accepted: 5 November 2021

1. Introduction

The predominant pattern for the rivers shape as natural systems is in the meandering plan. Basically, the flow structure in meanders is more complex than in straight-flow rivers. The main force acting on the flow in the bends is the centrifugal force which affects it when the flow enters the bend. This force changes the transverse slope of the water surface in the bend. Inequality of water depth in the outer and inner bends causes a lateral pressure gradient inside the bend. As the pressure gradient overcomes the centrifugal force, transverse flows are formed within the bend called secondary flows. By adding transverse secondary flows to the main flow along the path, a helical flow is formed in the bend. This helical flow plays the main role in the formation and development of bed changes as well as how the shear stress is distributed in the

[1] Department of Civil Engineering, Islamshahr Branch, Islamic Azad University, Islamshahr, Iran. Email: rasaei.iau@gmail.com **(Corresponding Author)**
[2] Department of Civil Engineering, Rudehen Branch, Islamic Azad University, Rudehen, Iran.

channel floor [1]. The presence of structures such as bridge piers within the bend affects the helical flow pattern in the bend and increases the complexity of flow behavior. In addition, by placing the bridge pier in the flow path due to changes in the flow structure, vortices are formed around the pier, which have been introduced as the main scouring factors around the bridge pier. Research shows that the horseshoe vortex in front and wake vortices on the pier behind are one of the important factors of creating scour around the bridge piers [2]. In Figure 1, the main vortexes are shown around a bridge pier.

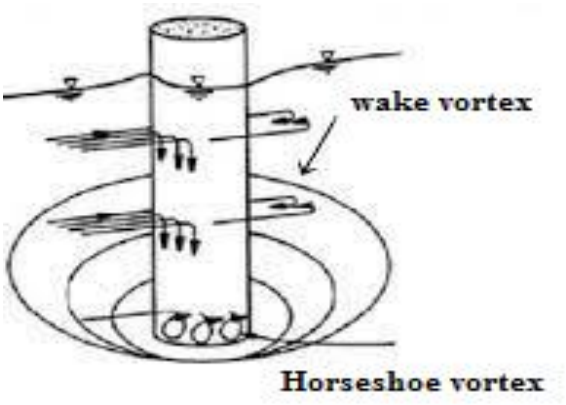

Figure 1. Schematic of the vortices formed around the pier

Many researchers from the past to the present with Laboratory and numerical methods and considering various parameters try to study the flow structure around The bridge piers were in straight and bended paths. Gargic and Bajestan [3] were investigated on the scour depth around the bridge, in the 90-degree bend. They concluded that scour depth becomes higher in the bend and increase the angle, so that it reaches the highest amount at a 90-degree angle. Hajebi and Meftah [4] examined the flow lines caused by scour around the piers using the SSIIM numerical model. They found that the flow lines around the square pier are like a circular pier. The results showed that the scour around the square pier is similar to the horseshoe, with the difference that the flow disturbance and the amount of scour are higher than the circular pier. In 2011, Masjedi et al. [5] Conducted experiments on the effect of the geometric shape of the bridge pier in control of local scour in the river bend. Their research showed that the maximum scour depth occurred on both piers in the first half of the bend and at a position of 14 degrees. Also, in all cases, the average of maximum scour depth around the cylindrical pier was observed compared to the square pier with a half-circle nose of 7% less. Karimi [6] examined the effect of bridge pier on depth and scour profile on rectangular and conical aerodynamics pier. He concluded that the pier shape will have a tremendous effect on the scour phenomenon, so that the aerodynamic bridge pier reduces the maximum scour depth respect to rectangular shapes. The measurements showed that the maximum scour depth around the aerodynamic pier of 47% less than the scouring around the rectangular pier. Yahyavi and Bakhshpuri [7] investigated the effect of cubic pier geometric shape and aerodynamics with different widths on local scouring. In 2009, Ismaili et al. [8] Using the SSIIM numerical model, simulated 3D scouring around the bridge pier. They found that the SSIIM numerical model could effectively simulate the flow of natural rivers. The results also showed that the k-ω model provides more reasoned results than other turbulence models. Elsaeed [9] investigated the validity of the SSIIM numerical program for calculating local scouring around bridge piers. He concluded that the SSIIM program is a

reliable and inexpensive tool that helps engineers and researchers to simulate and predict the amount of scour and sediment transport around bridge piers with great accuracy. Akib et al. [10] investigated the reinforcement of bridge piers against scour damage and compared them with the results obtained from the SSIIM program (Case study: Sufian- Marand braidge). While confirming the SSIIM numerical model in the simulation of scour around the pier, they proved that the height of the foundation should be considered more than the depth of scour. Feal et al. [11] investigated the effect of pier shape on scour depth. They reported that the pier shape of the bridge, like the river angle, should not be overlooked and has significant effects on scouring rates. Moustafa and Moussa [12] evaluated local scouring around the piers of Aswan and El Minia bridges using one-dimensional and two-dimensional mathematical models and concluded that the least scouring occurs in front of the sharp point of the bridge pier. In 2020, Rasaei et al. [13, 14 and 15] Conducted a numerical and laboratory study of local scouring around bridge piers located in a 90-degree convergent bend. Their results showed that the SSIIM numerical model is able to simulate the scour around the bridge piers properly and with minimal error.

Studies show that scouring research has been mainly on piers with simple shapes and in straight channels and less piers with aerodynamic shapes have been considered. Therefore, in this study, with the help of SSIIM three-dimensional numerical model, in addition to the use of aerodynamically shaped piers and its effect on scour, the effect of the river bend and the pier position at different angles of the bend have also been investigated.

2. Materials and Methods

2.1. SSIIM software and governing equations of the flow field

SSIIM[3] software was first developed by Mr. Olsen [16] at the Norwegian Institute of Technology in 1991 and developed in 2002. The SSIIM model solves the Navier-Stokes equations by default based on the standard k-ε turbulence model using a non-orthogonal non-displaced three-dimensional grid according to Equation 1. On the other hand, the volume control method is used for separation. The SIMPLE method is used to communicate the pressure and velocity terms in this software. it should be noted that in this model, the velocity field is calculated based on the implicit solution method and the velocity components are used in solving the transfer and diffusion equations for different sediment sizes.

$$\rho \frac{\partial U_i}{\partial t} + \rho U_j \frac{\partial U_i}{\partial Uj} = -\frac{\partial P}{\partial X_i} + \frac{\partial}{\partial X_j}(2\mu S_{ji} - \rho \overline{u_j' u_i'}) \quad (1)$$

In the above equation, the first and second sentences on the left are transient and transferable phrase, respectively. Also, the first sentence of the right parameter is defined pressure and the last sentence is the parameter related to Reynolds stresses.

2.2. Laboratory models and data

Because, the aim of this research is to simulate scouring around the piers of aerodynamic bridges located in different positions of a 90-degree bend. Therefore, the model, data and laboratory results of Ismail et al. [17] were used in the simulation process and validation of the numerical model. The pier used according to Figure 2 is aerodynamic cylinder which consist of a wide semicircular nose with a diameter of 10 cm and a narrow semicircular nose with a diameter

[3] Sediment simulation in intakes with multiply options

of 4 cm. In all cases, the pier was placed in the center of the channel bend. On the other hand, the range of change of parameters affecting scouring is presented in Table 1.

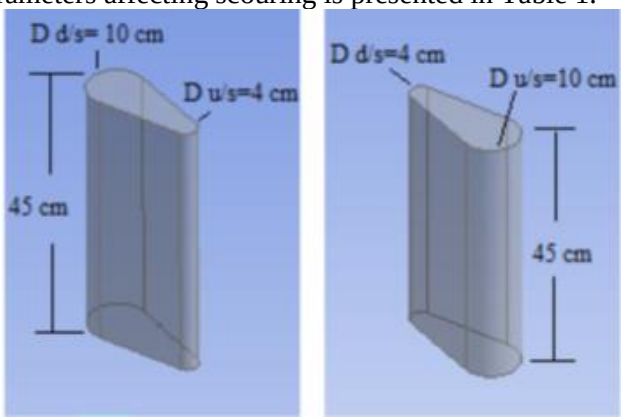

Figure 2. Aerodynamic pier [17]

Table 1. Range of effective parameters

Variable	Range
Discharge rate	58 L/S
pier position in the bend	30,60 and 90 degree
Depth of flow	120 mm
Sediment particle density	2.65
Average diameter of sediment particles.	1.45 mm

2.3. Production and regulation of field network

The channel used in this research is a flume with a 90-degree bend that consists of two straight channels with a length of 1m and a width of 0.8m, that are connected to the channel upstream and downstream (figure 3). The SSIIM program itself is not capable of generating geometry in complex simulations. For this purpose, with the help of MATLAB programming language, the necessary code was written to produce the network and model geometry. In order to increase the accuracy of the calculations, the geometry of the field was defined in such a way that the mesh size near the pier and inside the bend was considered smaller due to its more intense gradients.

In general, in the production process of field network, different meshes with the different sizes were tested for simulation at 90 ° bends. Finally, based on the results of mesh analysis, the geometry of the field was defined in such a way that for upstream and downstream channels, meshes with dimensions of 2∗2.5 cm were used. Also, meshes with a size of 2*3 cm were used to mesh the bended part of the channel. Figure 4 shows a schematic view of the networking used in numerical modeling.

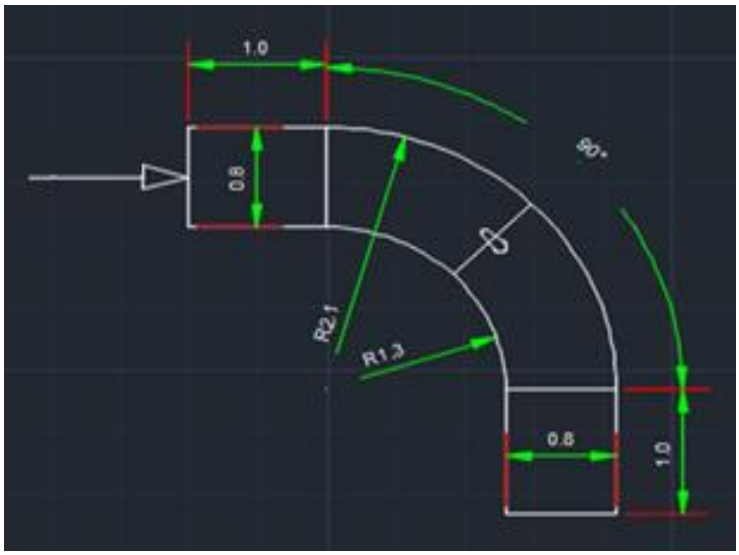

Figure 3. Plan of channel with 90-degree bend

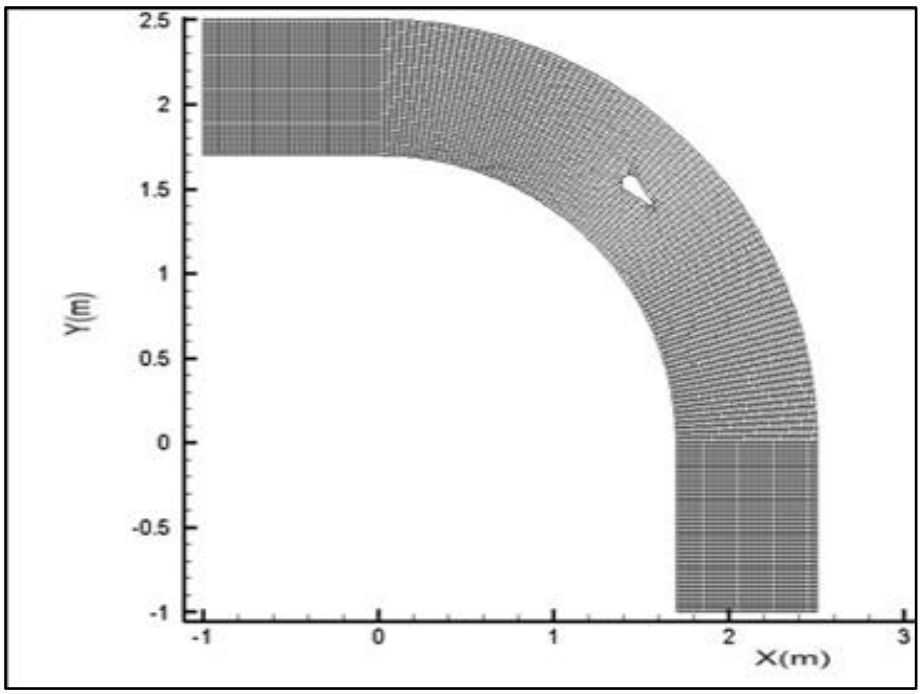

Figure 4. Schematic of field networking

3. Discussion and results

In this study, in order to investigate the effect of bend angle changes and pier aerodynamic shape on local scour, the pier was studied and simulated in the following six modes.

- Mode 1: the pier with a narrow nose in the upstream and a wide nose in the downstream and placed at an angle of 30 degrees.

- Mode 2: the pier with a wide nose in the upstream and a narrow nose in the downstream and placed at an angle of 30 degrees.
- Mode 3: the pier with a narrow nose in the upstream and a wide nose in the downstream and placed at an angle of 60 degrees.
- Mode 4: the pier with a wide nose in the upstream and a narrow nose in the downstream and placed at an angle of 60 degrees.
- Mode 5: the pier with a narrow nose in the upstream and a wide nose in the downstream and placed at an angle of 90 degrees.
- Mode 6: the pier with a wide nose in the upstream and a narrow nose in the downstream and placed at an angle of 90 degrees.

By placing the pier at angles of 30, 60 and 90 degrees of the bend and under the effect of a maximum flow rate of 58 L/S, the flow pattern including velocity, shear stresses and finally the maximum depth and volume of scour were studied and analyzed and finally compared.

3.1. Investigating the trend of changes in velocity vectors

Figure 5 shows the changes in flow lines within the bend and around the aerodynamic pier in all six modes. As an example in Figure (5a) we can see the flow lines extracted from the numerical model around the pier with a narrow nose in the upstream and at an angle of 30 degrees (mode 1). As can be seen in mode 1, the velocity decreases as the flow passes through the direct upstream channel and collision with the pier. As the flow passes through the pier, the flow velocity along the body increases again. As the flow reaches the downstream area and behind the pier, the speed decreases significantly again due to the creation of vortex flows. As the flow moves away from around the pier, it is observed that the flow lines in a regular, uniform, and developed form along the bend. It should be noted that in this mode, due to the low cross-sectional area at the upstream, the wake vortex flows are less intense in this area. In contrast, Figure (5b) shows the flow lines around the pier with a wide nose in the upstream and at a 30-degree angle (mode 2). Comparison of modes 1 and 2 shows that, with increasing diameter of the pier upstream, the flow velocity in collision with the pier and upstream decreases sharply. On the other hand, with decreasing the diameter of the pier downstream in mode 2, the flow velocity will increase more than in mode 1. The important point that can be seen in all cases is that with the entry of flow into the bend, the intensity of velocity vectors in the bend has increased significantly. Due to the high flow gradient at the edges of the bend and the creation of secondary flows, the lines intensity and consequently the flow velocity at the inner and outer edges of the bend has increased so that the highest velocity of the flow lines is observed in these areas.

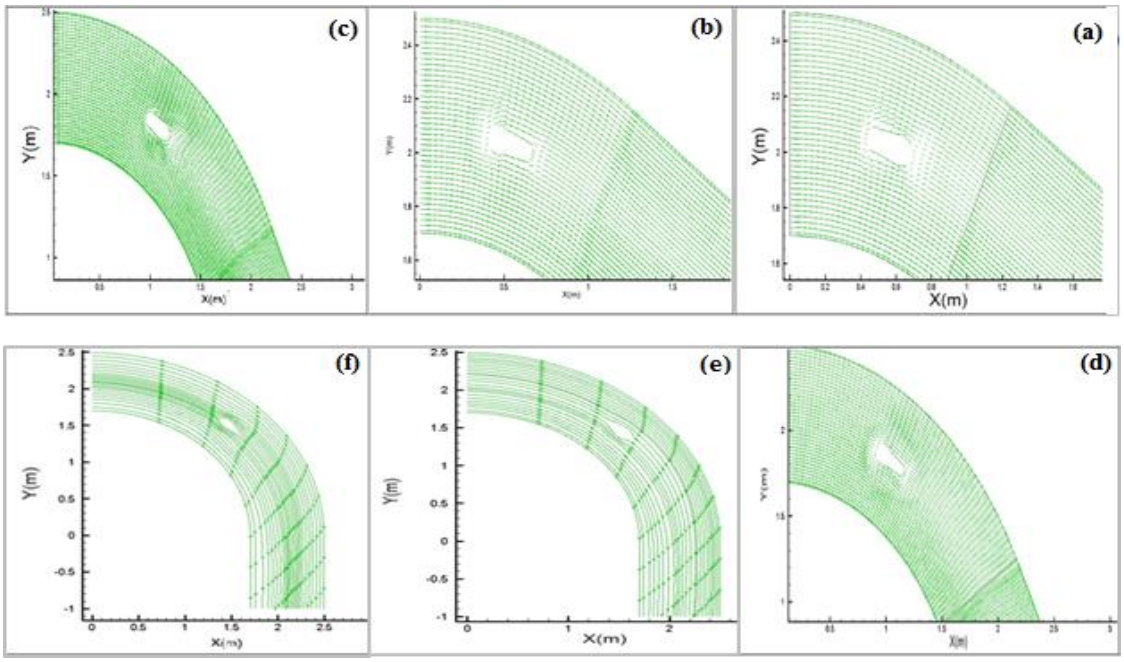

Figure 5. velocity line vectors. a) pier with an upstream narrow nose in an angle of 30 degrees; b) pier with an upstream wide nose in an angle of 30 degrees; c) pier with an upstream narrow nose in an angle of 60 degrees; d) pier with an upstream wide nose in an angle of 60 degrees; e) pier with an upstream narrow nose in an angle of 90 degrees; f) pier with an upstream wide nose in an angle of 90 degrees

Figure 6 also shows the maximum velocity changes around the aerodynamic pier in different positions. As can be seen, the maximum flow velocity increases with increasing position of the pier with an upstream narrow nose in the bend. On the other hand, with increasing the position of the pier with an upstream wide nose, the maximum flow velocity has decreased. Analysis of the results from the diagram in Figure 6 shows that the lowest flow velocity in all cases occurred at the collision point of the flow with the upstream narrow nose of pier in an angle of 30 degrees and at a rate of 0.7976 m/s. On the other hand, the highest velocity flows at the collision point of the flow with the downstream wide nose of the pier in an angle of 90 degrees and at a rate of 0.8649 m/s. It should be noted that in all modes, the maximum velocity around the pier with an upstream narrow nose is less than the pier with an upstream wide nose.

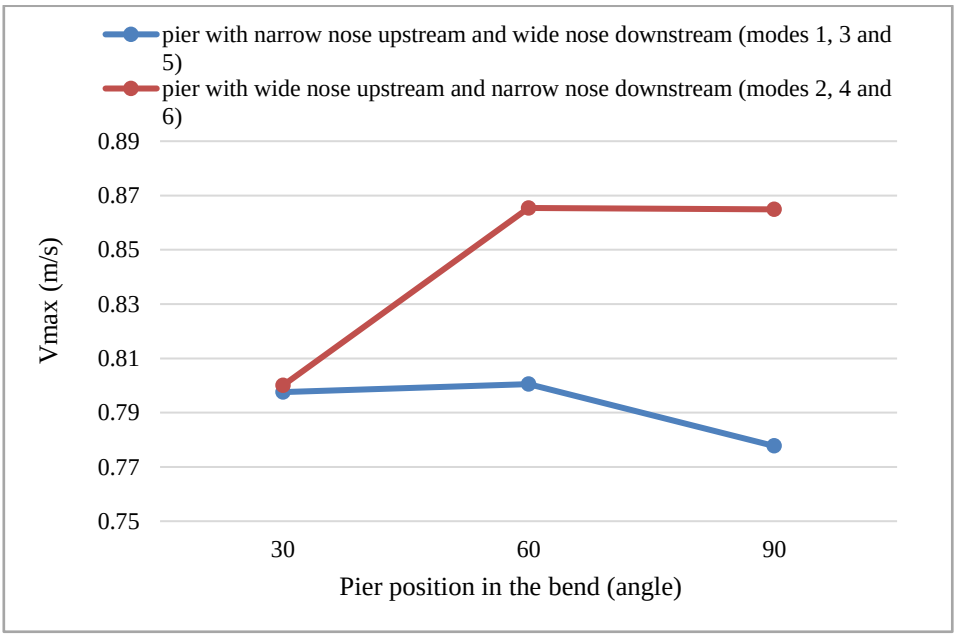

Figure 6. Diagram of maximum velocity Changes

3.2. Shear stress distribution

Figure 7 shows the distribution of shear stresses around the pier in all 6 modes. As can be seen, eddy flows are activated by placing the pier in the flow path and the flow colliding with the pier. As shown in Figure 7, depending on the shape and cross-sectional area of the pier in dealing with the flow, the intensity of shear stresses around the pier will also vary. The numerical model outputs show that in the case where the narrow nose of the pier is located in upstream, the intensity of shear stresses is much less than the pier whose wide part is located in upstream. This factor is certainly due to the aerodynamic shape and low cross-sectional area in collision with the flow. Also, the accuracy in the images of shear stresses output from the numerical model in Figure 7 shows that in all cases, due to the aerodynamics of the pier, the amount of shear stresses on the pier sides has decreased significantly. It should be noted that due to the secondary and eddy flows created in the bend, the maximum shear stresses were observed along the bend at the inner and outer edges of the bend.

Figure 8 shows a diagram of shear stresses changes around the pier in different positions. As can be seen in modes 1, 3 and 5, the intensity of shear stresses around the pier is less than the stresses created in modes 2, 4 and 6. In general, the results of modeling in Figure 8 show that in all modes, the maximum shear stresses around the pier with a wide nose at the upstream and at an angle of 60 degrees (mode 4) was 13.2031 N/m^2. On the other hand, the minimum shear stresses occurred around the pier with a narrow nose at the upstream and at an angle of 60 degrees (mode 3) at a rate of 7.48 N/m^2.

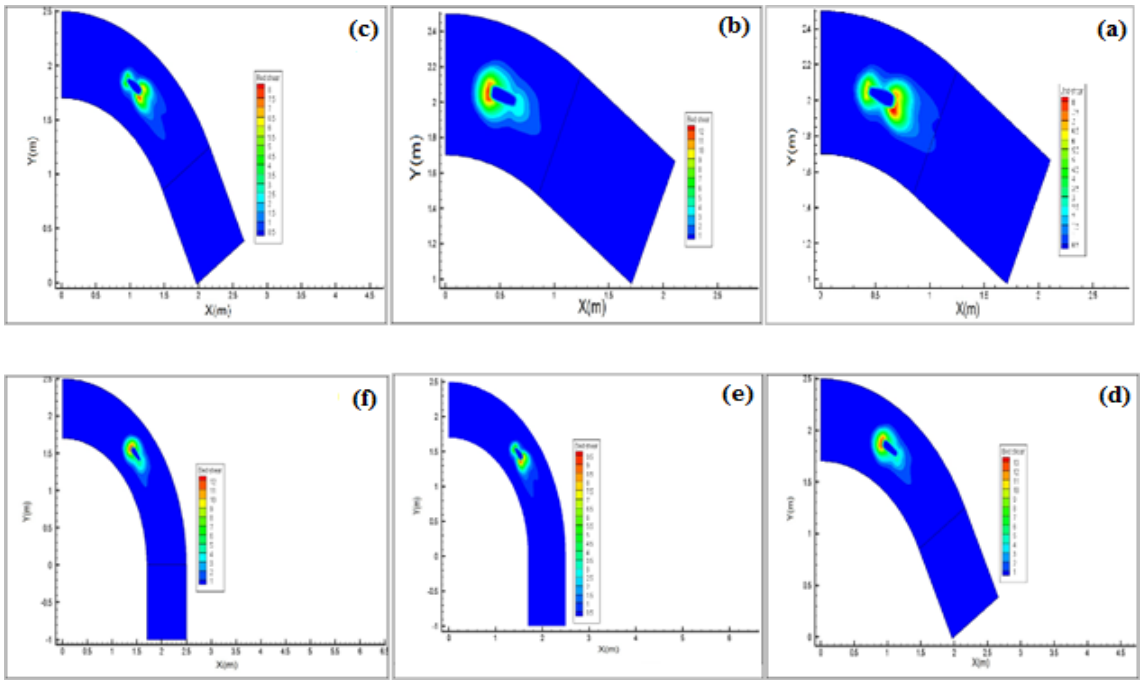

Figure 7. shear stresses Changes around the pier. a) pier with an upstream narrow nose in an angle of 30 degrees; b) pier with an upstream wide nose in an angle of 30 degrees; c) pier with an upstream narrow nose in an angle of 60 degrees; d) pier with an upstream wide nose in an angle of 60 degrees; e) pier with an upstream narrow nose in an angle of 90 degrees; f) pier with an upstream wide nose in an angle of 90 degrees

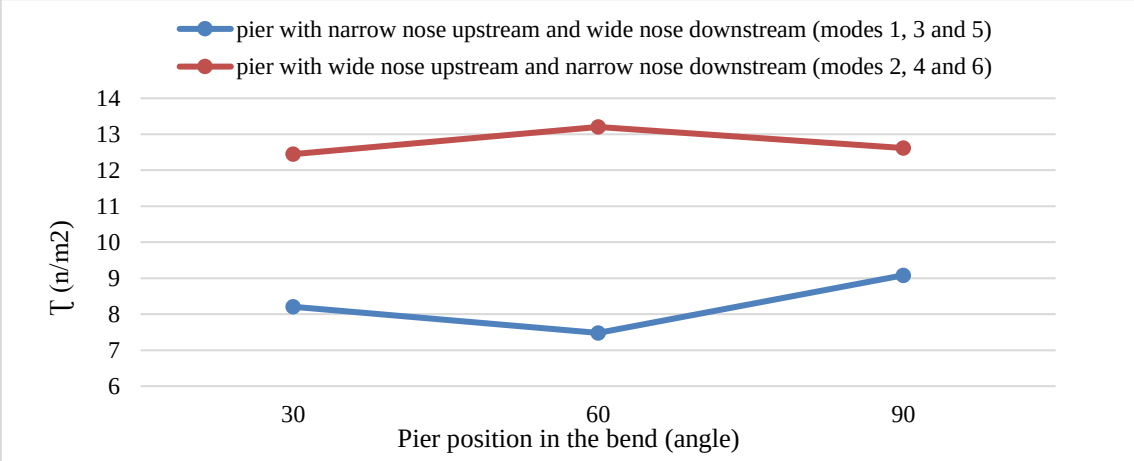

Figure 8. Diagram of maximum shear stresses Changes

3.3. Maximum depth and valume scour

The numerical model outputs show that the aerodynamic shape of the pier and pier position at different angles of the bend has changed the flow pattern so that it has a significant effect on both the bed topography and the maximum depth and volume of scour around the pier.

Figure 9 shows the scour hole around the piers at different angles of the 90 ° bend. According

to Figure 9, it can be seen that whenever the pier with a narrow nose is located in upstream, the depth and dimensions of the scour hole are less estimated. This factor is due to the low upstream cross section in the collision with flow, which leads to a reduction in shear stresses and thus a reduction in the depth and dimensions of the scour hole around a pier. On the other hand, it is observed that at low angles and especially in the first half of the bend, shear stresses are minimal and scour around the piers is negligible. Then, with increasing angle and entering the second half of the bend, the strength of the secondary flows and the shear stresses of the floor reach their maximum value. Tables 2 and Figures 10 and 11 show the changes in the maximum depth and volume of scour around a pier in different modes. As can be seen, in all modes, with increasing the pier position in the bend, the maximum depth and volume of scouring also increases. On the other hand, the volume of scouring around the piers with a wide nose upstream is far more than the volume of scouring around the piers with a narrow nose upstream in the same position. The results and calculations obtained from the numerical model outputs show that the maximum depth and volume of the scour hole when placing the pier with a wide nose at the upstream and at a 90-degree angle are estimated at 0.1197 m and 0.0844 m3, respectively.

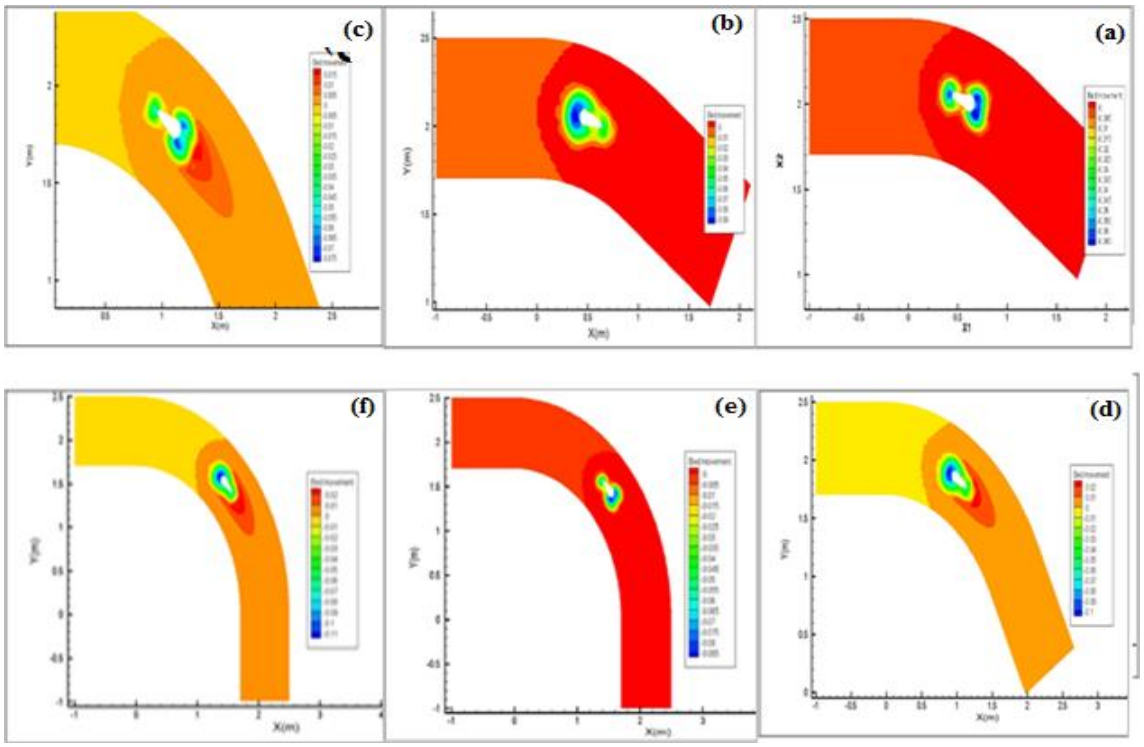

Figure 9. Scouring hole around the pier. a) pier with an upstream narrow nose in an angle of 30 degrees; b) pier with an upstream wide nose in an angle of 30 degrees; c) pier with an upstream narrow nose in an angle of 60 degrees; d) pier with an upstream wide nose in an angle of 60 degrees; e) pier with an upstream narrow nose in an angle of 90 degrees; f) pier with an upstream wide nose in an angle of 90 degrees

Table 2. Values of maximum depth and volume of scour in all modes

Aerodynamic shape of pier \ Angle		30	60	90
pier with narrow nose upstream and wide nose downstream (modes 1, 3 and 5)	Maximum scour depth	-0.0714	-0.076	-0.0890
	Maximum scour volume	-0.0466	-0.0506	-0.0532
pier with wide nose upstream and narrow nose downstream (modes 2, 4 and 6)	Maximum scour depth	-0.103	-0.111	-0.12
	Maximum scour volume	-0.0722	-0.0771	-0.0844

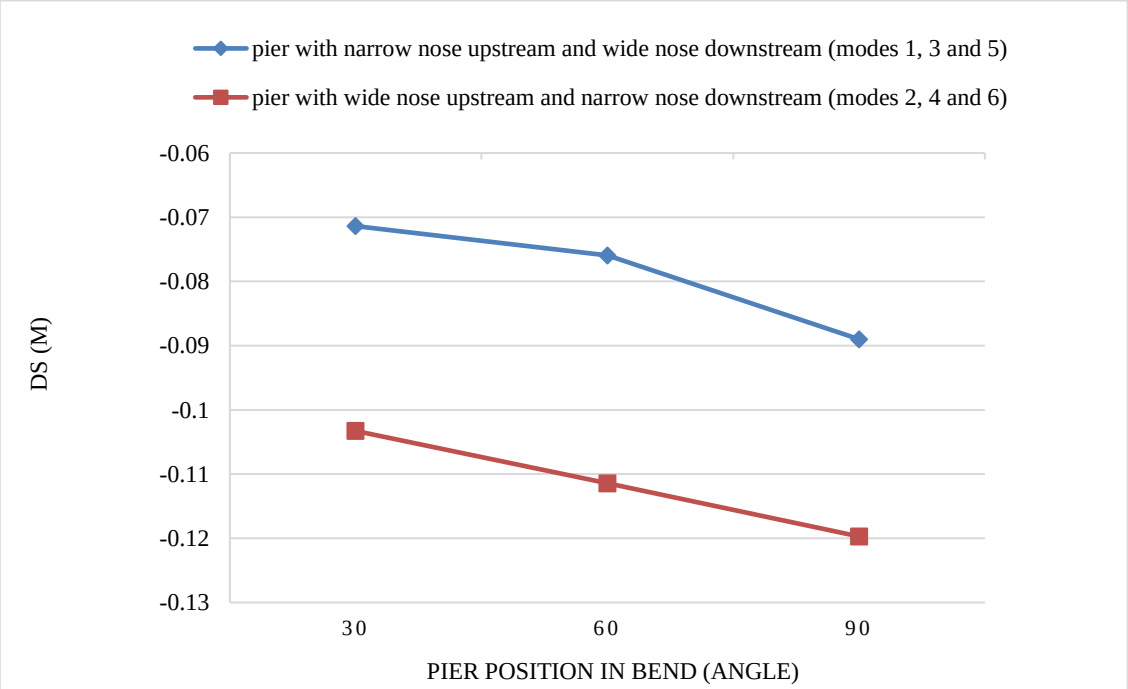

Figure 10. Changes of the maximum scour depth

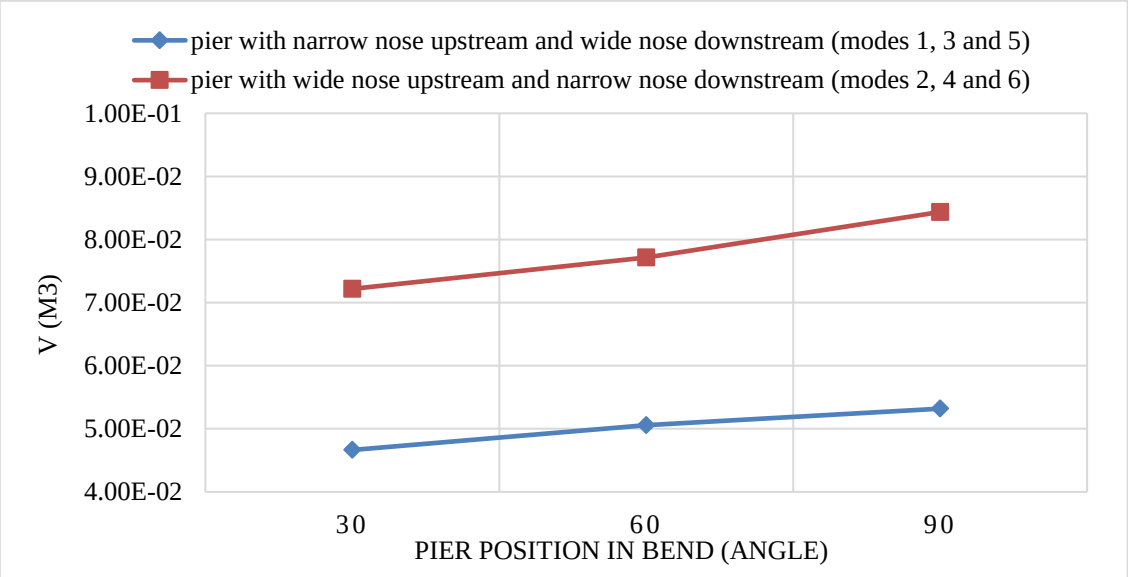

Figure 11. Scour volume changes

4. Conclusion

- In all modes, with increasing the pier position in the bend, the maximum depth and volume of the scour hole has increased. The maximum and minimum depth and volume of the scouring hole around the pier occurred at 90 and 30 ° angles, respectively.
- The aerodynamic shape of the pier has a significant effect on the depth and volume of scour around the pier. In all modes, the depth and volume of the scour hole around pier with a narrow nose upstream was less estimated.
- The maximum volume of scour occurred in the second half of the bend and mainly in the angle range of 60 to 90 degrees.
- In all modes, maximum shear stresses occurred when the wide nose of the pier was in upstream.
- When the narrow nose of the pier was in upstream, the maximum amount of shear stress occurred at a 90-degree angle.
- When the wide nose of the pier was in upstream, the maximum amount of shear stress occurred at a 60-degree angle.
- In all modes, the maximum horizontal velocity in the bend occurred at an angle of 30 degrees.
- The results of the numerical model show that SSIIM software has an appropriate and acceptable ability to simulate scour around bridge piers.

References

1. Rozovskii I.L, (1957). Flow of water in bend of open channel, Academy of Sciences of the Ukrainian SSR, Institute of Hydrology and Hydraulic Engineering.
2. Melville B W, Raudkivi A J, (1977). Flow Characteristics in Local Scour at Bridge Piers. Am.Soc. Civ. Eng., J.Hydr. Engrg, 15(4): 373-380.

3. Gargic V, Bajestan M S, (2011). Investigating the scour depth around the bridge rationale in the 90-degree arc. Sixth National Congress on Civil Engineering (in Persian).
4. Hajebi_F, Meftah M, (2013). Investigation of flow lines due to scour around the bridge pier using SSIIM numerical model. 9th International River Engineering Conference (in Persian). Shahid Chamran University, Ahvaz. Iran.
5. Masjedi A R, Telvari A R, Kazemi H, (2013). Laboratory investigation of basic geometry of the bridge on scour control around the river bend. Watershed Engineering and Management (in Persian), 4(4): 208-2166.
6. Karimi O, (2013). Investigation of the effect of bridge base shape on depth and scour profile around it. 4th Conference on Water, Wastewater and Waste Management (in Persian), Tehran, Iran.
7. Yahyavi S, Bakhshpuri Y, (2015). Evaluating the effect of the geometric shape of the bridge pier on the scouring around it. Shahid beheshti university. Tehran, Iran, (in Persian).
8. Esmaeili T, Dehghani A A, Zahiri A, Suzuki K, (2009). 3D Numerical Simulation of Scouring Around Bridge Piers (Case Study: Bridge 524 crosses the Tanana River). World Academy of Science, Engineering and Technology, 58(10): 1028–1032.
9. Elsaeed G H, (2011). Validating SSIIM 3-D Numerical Model to Calculate Local Scour around Bridge Piers. INTERNATIONAL JOURNAL of ACADEMIC RESEARCH, 3(3): 501–505.
10. Akib SH, Basser H, Karami H, Jahangirzadeh A, (2016). Retrofitting of Bridge Piers against the Scour Damages: Case Study of the Marand-Soofian. International Journal of Computational Science and Engineering 8(1):56-60.
11. Fael C, Lança R, Cardoso A, (2016). Effect of pier shape and pier alignment on the equilibrium scour depth at single piers. International Journal of Sediment Research, 31(3), 244–250.
12. Moustafa A, Moussa A, (2018). Evaluation of local scour around bridge piers for various geometrical shapes using mathematical models. Ain Shams Engineering Journal, 9(4), 2571–2580
13. Rasaei M, Nazari S, Eslamian S, (2020). Experimental investigation of local scouring around the bridge piers located at a 90° convergent river bend. Sadhana, 45(1), 87.
14. Rasaei.M, Nazari S, Eslamian S, (2020). Experimental and numerical investigation the effect of pier position on local scouring around bridge pier at a 90° convergent bend. Journal of hydraulic structures, 6(1): 55-76.
15. Rasaei.M, Nazari S, Eslamian S, (2020). Experimental and Numerical Investigation of Local Scouring around Bridge Piers in Different Geometric Shapes at a 90° Convergent meander. Journal of hydraulic structures, 6(2): 55-76.
16. Olsen N R B, (2004). CFD Algorithms for Hydraulic and Sedimentation Engineering. The Norwegian University of Science and Technology.
17. Ismael A, Gunal M, Hussein H, (2015). Effect of Bridge Pier Position on Scour Reduction According to Flow Direction. Arabian Journal for Science and Engineering, 40(6): 1579–1590.